Proceedings of the International Conference on Manufacturing Systems – ICMaS

University POLITEHNICA of Bucharest, Machine and Manufacturing Systems Department
Bucharest, Romania

3-D RESEARCH ON FORK ARMS OF FORKLIFT TRUCKS

Yanko SLAVCHEV

Abstract: *This article presents a research, conducted by 3-D computer models and the finite element method (FEM), on the stressed state of fork arms of forklifts. Several modes of attachment to the carrying plate have been taken into consideration. Special interest has been paid to the stressed state of the folded region and the console welds for arms attachment. A multi-objective optimization, specifically a goal driven optimization (GDO), is performed to estimate the length of the fork arm when it is loaded by a payload, placed on a wooden pallet.*

Keywords: *3D computer model, FEM, curved beam, fork, optimization, wooden pallet.*

1. INTRODUCTION

The fork is the most popular removable equipment item of the fork lift trucks. It consists, most commonly, of two arms attached to the carrying plate of the fork lift truck. Attaching is either by a welded upper console support or by connecting holes.

The welded console-supported forks are widespread in practice. The fork arm has a folded (or bent region), due to material roughing which is applied in order to strengthen the bent cross-section.

Fig. 1 shows a typical fork arm, modes of attachment and primary dimensions.

Dimensions h, b, t according to DIN regulations and h^*, b^*, t^* according to ISO regulations are considered as the primary dimensions of fork lift arms attachment. There are two basic types of forks according to the dimension b: forks of low, $b \leq 80$ mm and high hanging $b > 80$ mm.

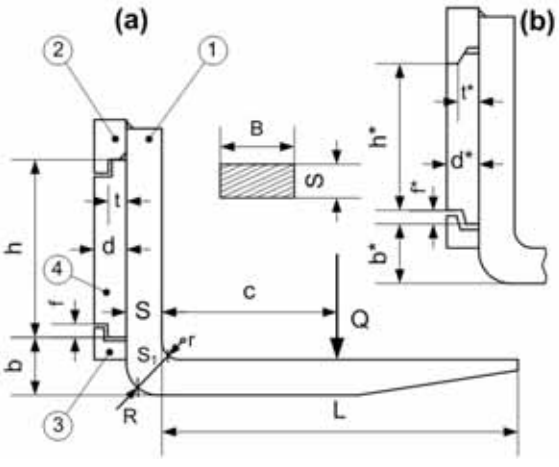

Fig. 1. A fork lift arm:
1 – fork arm; 2 – carrying (upper) console; 3 – limiting (lower) console; 4 – carrying plate; B and S – width and thickness; (a) DIN mode of attachment; (b) ISO mode of attachment; S_1 – folded region thickness; r and R – folded region radii; L – length of the working area; h, d, f and h^*, d^*, f^* – carrying plate parameters.

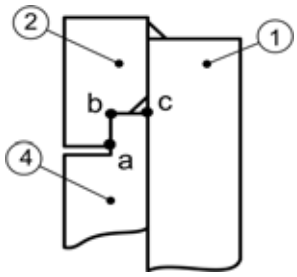

Fig. 2. Contact between 2 and 4 according to DIN.

The stressed-state problems of fork-lift arms, due to the particularity of the bent region, the modes of attachment to the carrying plate, as well as the loadings, are not studied as much.

The objective of the current article is to perform a more extensive scientific research of the abovementioned problems. The research, conducted through the use of CAD models and the FEM aims at drawing certain recommendations concerning the design calculation and optimization procedures for fork-lift arms.

2. MODEL STUDIES, RESULTS AND ANALYSES

2.1. 3-D model generation

A fork lift arm is modeled as a 3D object [6] and meshed. The following is considered, Fig. 1:

- part 1 is in contact with parts 2, 3 and 4; parts 2 and 3 are welded to 1; contact between parts 4 and 1 is not idealized allows for contact separation due to part 1 deformation, i.e. contact status non-linearity is permitted [2], 3];
- contact between 2 and 4 according to DIN (Fig. 2) and ISO (Fig. 3) is along planes *ab* and *bc* allowing frictional type contact; the bc plane slope with respect to the vertical is $\alpha = 20°$ the ISO mode;
- the carrying plate 4 is rigid and remains always fixed;
- loading Q is a concentrated force, defined in the plane of symmetry and distance c depends on the radius r;
- fork material is steel;

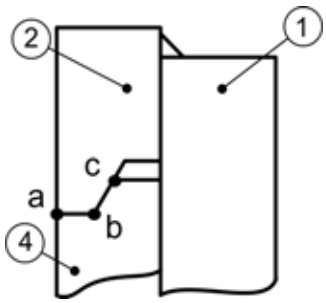

Fig. 3. Contact between 2 and 4 according to ISO.

The FE mesh implements the established default global settings based on the physics preference, which is mechanical, for the current simulation. The selected meshing algorithm is patch conforming.

The element type is a higher order 3D 20-node hexahedral solid element that exhibits quadratic displacement behavior [1].

A mapped meshing control is applied so as to produce a structured mesh [6] that provides a more consistent representation at the walls and the folded region, Fig. 4, and ensures mesh consistency throughout the volume.

The console welds, present in the model, are meshed with 20 node quadratic wedge elements. Quadratic quadrilateral contact and target elements (a total of ≈1 500) are used to define the contacts. This type of elements offers 8 nodes and assumes the parameters of the solid element it is attached to. To simplify the analysis, areas that are not subject to this study – contacts between the lower support and the fork arm, are defined as being in bonded type contact.

On one hand, it helps not to overload the hardware with excessive calculations and on the other hand it attains a theoretical contact on the entire contacting surface without any initial penetrations. The fork arm mesh is checked for validity and the following values are obtained: Jacobian ratio: 1÷2, parallel deviation: 0÷10°, max structural error≈1.3e^{-2}J.

The mesh is well-structured [1].

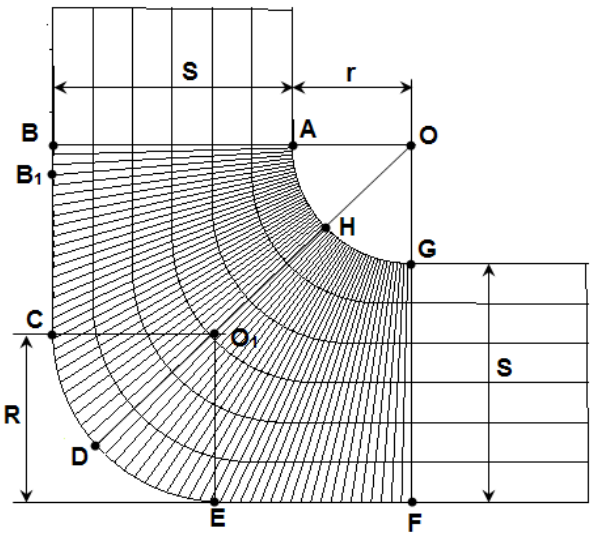

Fig. 4. Mapped mesh of the folded region.

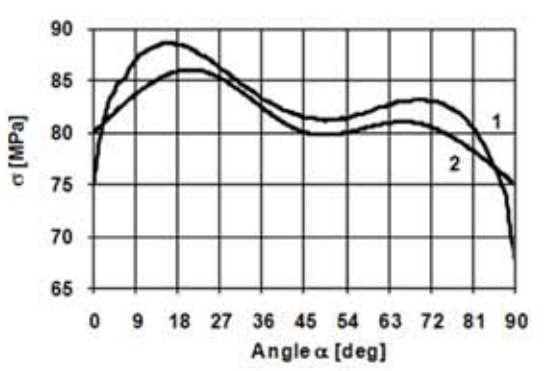

Fig. 5. Stresses in the *AHG* zone of the folded region 1 – 3D von-Mises; 2 – strain-gauging.

2.2. 3-D model analyses

FE analysis is conducted of a fork arm with the following parameters, Fig. 1: B = 104 mm, S = 40 mm, $S1$ = 53 mm, r = 20 mm, R = 28.62 mm, Q = 4500 N, c = 400 mm, b = 80 mm. Figure 5 presents stresses within the *AHG* zone of the central cross-section of the fork arm obtained from the 3-D model and stresses from measurements (strain-gauging).

Figure 6 shows equivalent stress distribution within the *BCDEF* zone of central cross-section of the fork arm.

The outer radius R is determined through a relation based on the geometry from Fig. 4 as follows:

$$R = \frac{S\sqrt{2} - S_1}{\sqrt{2} - 1} + r\,. \tag{1}$$

It follows from the analysis that the max stresses occur at the inner side of the folded region.

It is established that the stresses from the measurements have similar behavior to the stresses from the 3-D model. The estimated error between the von-Mises gauged and model stresses is in the range 2÷3%.

Stresses on the outer side of the folded region are much smaller than those on the inner side.

The lowest point of the contact between the console 3 and the fork-arm 1 is denoted by B_1.

It is estimated that in point B_1, Fig. 4, there occur local extreme stresses as shown on Fig. 6.

Stresses then start decreasing. The min stresses occur at section angle of 45deg.

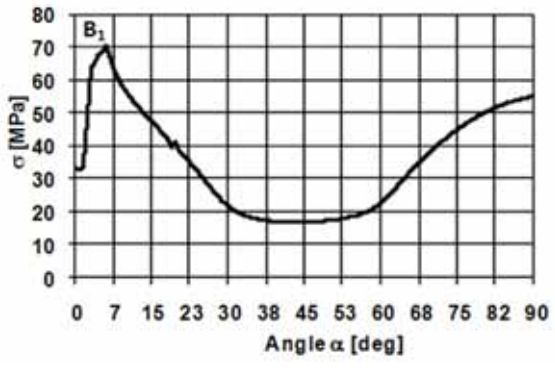

Fig. 6. Stresses in the BCDEF zone of the folded region.

Table 1

Q [kN]	*B* [m]	*S* [m]	S_1 [m]	*h* [m]	*d* [m]	*t* [m]
1.94	0.10	0.04	0.05	0.4	0.025	0.020
30	0.14	0.05	0.06	0.4	0.030	0.025
45	0.14	0.06	0.07	0.4	0.040	0.025

*Note: Parameter f = 15 mm for all Q

Similar studies are performed for fork-arms of capacities 12.5 kN, 20 kN and 30 kN. The fork-arm parameters are listed in Table 1.

3. INFLUENCE OF THE MODE OF ATTACHMENT ON THE STRESSED STATE OF THE FORK ARM

Stresses in forks of low and high hanging (according to DIN and ISO) are studied.

The stressed state of 20kN lift capacity fork arms is studied for two cases – of low (b = 76 mm) and high (b = 160 mm) hanging. It is established for the low case forks that: the stresses at the rear of the fork arm, from the contact with the bottom edge of plate 4 (dimension b, Fig. 1) to the bottom of console 3 (point B_1), decrease by ≈50% and after that become equal to the stresses of a high case fork arm; the folded region max tension stresses have smaller values by 1.5÷2 %. Moreover, stresses in the mid cross-section of the fold ($\alpha = 45°$) of the low hanging case, have smaller values by 3÷4 %. It is due to the structure limitations since the outer radius R of the low case tends to r and as a result, the thickness S_1 gains max value.

$$S_1 = S\sqrt{2}\,. \tag{2}$$

It is obvious that the low hanging case of fork arms has weak influence on the stressed state of the folded region. The stressed state within the area of attachment is determined by an FE and strain-gauge study of the welds, Fig. 7, of a fork arm with DIN attachment and loading Q = 1.94 kN.

Welds mesh is checked for validity and the values are as follows: Jacobian ratio≈1, parallel deviation≈0°, max structural error≈4e^{-4} J. The mesh is well-structured.

The frictional type of contact, that the simulation accounts for, makes the problem a non-linear one. The friction coefficient is assumed to be in the range 0.1÷0.2.

A direct solver type is used and convergence is attained after 11 iterations.

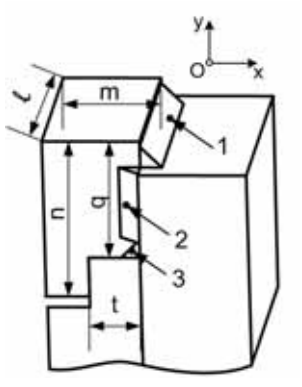

Fig. 7. Studied welds.

Table 2

№	Experiment [MPa]	FEA [MPa]
1 (σ_x/σ_{Eq})	–76	–77.5/91.4
2 (σ_x/σ_{Eq})	–11	–8.7÷42.1/49.9
3 (σ_{Eq})	-	144.7

The parameters of the mode of attachment are: weld leg 8 mm; lengths of welds 1, 2, 3: l_1 = 80 mm, l_2 = 27 mm, l_3 = 80 mm; l = 80 mm; m = 36 mm; n = 60 mm; q = 45 mm; t = 20 mm;

Weld stresses are measured at points 1, 2 and 3, as shown in Fig. 7.

The FEA and experimental (strain-gauging) results are listed in Table 2.

The computer model confirms the experimentally obtained normal stress values for points 1 and 2. Point 2 stresses vary in the range –8.7÷42.1 Pa. The equivalent stress value for point 3, from the interior weld, is also listed, but it is quite hard to receive a value by an experimental study. The same is accomplished for points from the other two welds.

Similar model studies are carried out for the ISO mode of attachment preserving the weld parameters (weld leg and length) and loading values the same as for the DIN mode. The carrying console parameters are t^* = 19 mm, m^* = 25 mm, f^* = 14 mm respectively, while these of the carrying plate are h^* = 380 mm, d^* = 19 mm; the width and thickness of the fork arm as well as the thickness of the folded region of the fork arm are the same as in Table 1.

It is observed that in this case the equivalent stresses of the ISO mode of attachment increase, in comparison with the DIN mode, as follows: for weld1 by 4.8 %, for weld2 by 12 % and for weld3 by 13 %.

It is obvious that the DIN mode of attachment is more suitable regarding the safety of the carrying unit.

4. OPTIMIZATION OF THE WORKING LENGTH *L*

The working length studies of the fork lift arm take into account the actual loading during exploitation. The payload is assumed to be placed on a 1000 × 1000 mm wooden pallet, which is situated eccentrically on the fork. The lift capacity is $Q_n = 12.5$ kN and a dynamic factor is accounted for. Loading on a single fork arm is

$$Q = k_{dyn} k_f Q_n\,, \tag{3}$$

where $k_{dyn} = 1.2 \div 1.8$ is the dynamic factor and $k_f = 0.66$ accounts for the eccentric loading.

The pallet material is orthotropic with linear properties: modulus of elasticity along the fibers E = 1 177.8 MPa and across the fibers E = 686.5 MPa; shear modulus G = 540 MPa; Poisson's coefficient μ = 0.

A goal driven optimization (GDO) is used [4], [5] with two input parameters – the dynamic factor k_{dyn} and the length L, and one output parameter – the equivalent stress $\sigma_{Eq,P}^{\max}$ in the pallet (point P above the fork arm tip, Fig. 8).

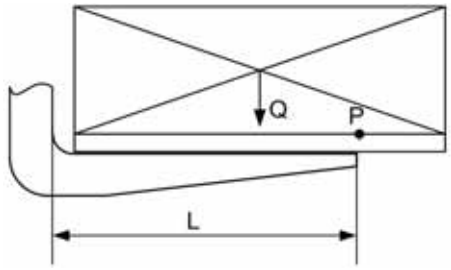

Fig. 8. Point P above the fork arm tip.

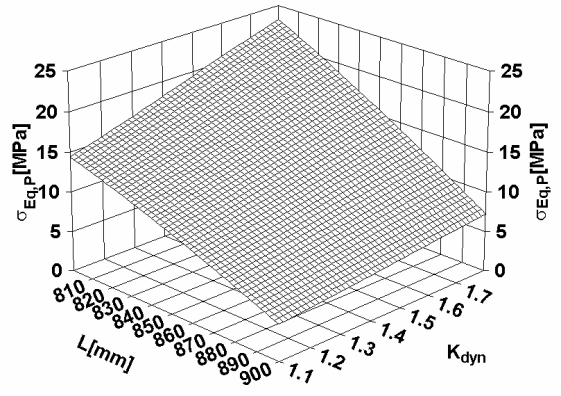

Fig. 9. A set of design points.

A set of design points, Fig. 9, is generated by a series of FE analyses, where each point is defined by three coordinates $\left(L; k_{dyn}; \sigma_{Eq,P}^{\max}\right)$.

The optimization helps determine those optimum points from the set that fulfill the constraints:

$$\sigma_{Eq,P}^{\max} < 11 \text{ MPa} \; ; \; k_{dyn} \in [1.2; 1.8] \; ;$$
$$L_{dyn} \in [800; 900] \; ; \; L \to 800 \text{ mm} . \qquad (4)$$

Several optimal cases are obtained. Case with coordinates (L 850 mm; $k_{dyn} = 1.23$; $\sigma_{Eq,P}^{\max} = 10.95$) is selected since it falls in a recommended series of lengths at a step of 50 mm.

5. CONCLUSIONS

Similar optimizations of the length L could be utilized for forks of different load capacities.

There have been created 3D computer models. Employing the FEM, these models help study the stressed state of the folded region of fork arms for different load capacities and modes of attachment. The model results are proved by corresponding strain-gauging measurements.

A method is proposed for calculating the optimal working length of fork-arms of fork-lift trucks.

REFERENCES

[1] *** (2007). ANSYS, *Theory reference*.
[2] Parisch, H., *A* (1998). *Consistent Tangent Stiffness Matrix for Three-Dimensional Non-Linear Contact Analysis*, International Journal for Numerical Methods in Engineering, Vol. 28, pp. 1803−1812.
[3] Peric, D. and Owen, D.R.J. (1992). *Computational Model for 3-D Contact Problems with Friction Based on the Penalty Method*, International Journal for Numerical Method in Engineering, Vol. 35, pp. 1289–1309.
[4] Sawaragi, Y.; Nakayama, H. and Tanino, T. (1985). *Theory of Multiobjective Optimization*, Vol. 176 of Mathematics in Science and Engineering, Academic Press Inc., Orlando, FL.
[5] Steuer, R.E. (1986). *Multiple Criteria Optimization: Theory, Computations, and Application*, John Wiley & Sons, Inc, NY.
[6] *** (2007). *SolidWorks, Reference Guide*.
[7] Zienkiewicz O.C., Taylor R.L., Zhu J.Z. (2005). *The Finite Element Method: Its Basis and Fundamentals*, Elsevier, NY.
[8] Zahavi E., Barlam D. (2001). *Nonlinear Problems in Machine Design*, CRC Press, NY.

Author:

PhD, MEng, Yanko SLAVCHEV, Assistant Engineer; Technical University of Sofia, Faculty of Mechanical Engineering, Engineering Logistics, Materials Handling and Building Machines,
E-mail: ya_slavchev@abv.bg